Enhanced mechanical strength and ductility of metal-repaired defective carbon nanotubes: A density functional study

G. P. Zheng[a] and H. L. Zhuang
Department of Mechanical Engineering, Hong Kong Polytechnic University, Hung Hom, Kowloon, Hong Kong 10000, Hong Kong

(Received 7 March 2008; accepted 18 April 2008; published online 12 May 2008)

Metal atoms are filled into the defective sites of single-walled carbon nanotube (SWCN) containing vacancy defects, resulting in a stable repaired SWCN. The tensile deformation of the repaired SWCN is investigated by spin-polarized density functional theory. Compared to the defective SWCN, the repaired CN shows significant enhancements in mechanical strength and ductility that are close to those of pristine CN. The underlying physics of these behaviors are analyzed by the structural transformation, electronic structures, and spin and charge distributions during the tensile tests. A strong magnetomechanical coupling effect is found to be responsible for the enhanced mechanical behaviors of metal-CN hybrid structures. © *2008 American Institute of Physics*. [DOI: 10.1063/1.2924275]

Because of the fact that the ideal Young's modulus, mechanical strength, and strength-to-density ratio of carbon nanotubes (CNs) are unparalleled by any other materials available to date, CNs are considered as excellent structural materials in automobiles, aerospace, and even hypothetically considered to be used as space elevator. However, several types of intrinsic defects exist and, in fact, the defect concentration of CN is at least one defect per 4 μm.[1] The mechanical strength and ductility of CN can be significantly lower than those of an ideal one.[2] Hence, the benefits of the excellent mechanical properties of CNs may be lost. Defective CNs can be repaired by organic molecules[3] or intertube cross-linking[4] but the mechanical behaviors of such repaired CNs may not be compatible with those of the pristine ones.[5] Transition metals can be considered to repair the defective CN since *p-d* hybridization between metal and carbon results in a strong and stable hybrid structure, which is similar to metal carbide in bulk structure.

On the other hand, CN metal matrix composite has attracted attention[6,7] in the past decade because of the scientific and engineering needs for the strengthening of metals and alloys. However, the binding energy between metals and pristine CN is rather small,[8] resulting in a poor metal-CN adhesivability. Defective CNs consisting vacancy defects may be promising reinforcements since the dangling bonds around the vacancies can provide active sites for metal-CN interaction and the mechanical properties of such hybrid structure have to be investigated.

In this study, we select a defective (5,5) single-walled (SW) CN consisting of a monovacancy. The 3*d* transition-metal adatoms or clusters are placed around the vacancy site, simulating the repair of defective CN by metal coatings. Our calculation is based on the spin-polarized density functional theory. The calculation is carried out by using the VASP code[9] with projector-augmented plane wave potentials.[10] The pristine SWCN supercell consisting of 120 atoms is shown in Fig. 1(a). Periodic boundary condition is employed along the axis. The defective SWCN consisting of a vacancy can be constructed by removing a carbon atom labeled as D from the sidewall, corresponding to a defect concentration of 0.84 at. %. To simulate the repair of defective CN using 3*d* transition metals, we place one cobalt atom or a ring of ten cobalt atoms near the defective sidewall. Firstly, we allow the reconstruction to occur for defective SWCN only, resulting in a stable defective SWCN. We found that the defective CN reconstructs into "perpendicular" BC bonding configuration [Fig. 1(d)] with a vacancy formation energy of 5.54 eV, which is the most stable structure in (5,5) SWCN with a monovacancy.[11] Then, the hybrid structure consisting of such stable defective CN and cobalt atoms shown in Fig. 1(b) or Fig. 1(c) is subjected to further relaxation, leading to a stable metal-CN hybrid structure. Because we have found that the mechanical properties of metal-CN hybrid structures consisting of one cobalt atom and a ring of ten atoms are similar, in what follows, we only present the deformation behaviors of defective SWCN repaired with one cobalt atom. The equilibrium structure of a defective (5,5) SWCN repaired with one cobalt atom is shown in Fig. 1(e). The hybrid structure has two carbon-cobalt bonds and is denoted as CN-X1. The cobalt binding energy of such hybrid structure is defined as $E_b=E_D+E_{\mathrm{Co}}-E_{\mathrm{CN\text{-}X1}}$, where E_D is the total energy of defective CN. $E_{\mathrm{CN\text{-}X1}}$ is the total energy of CN-X1 and E_{Co} is the total energy of a spin-polarized cobalt atom. $E_b=6.90$ eV and is much larger than that (1.9 eV) of pristine SWCN with a cobalt adatom,[12] suggesting a successful repair of the defective SWCN using transition-metal atoms or clusters.

Uniaxial tensile strains are applied to the metal-CN hybrid structure. Figures 1(f) and 1(g) show the structures of hybrid structure and defective CN under various tensile strains, respectively. The instability of defective CN occurs when the vacancy defect starts to evolve at a strain of 12% by the breaking of a bond along the axis direction (the "parallel" bond) close to the vacancy site. In metal-CN hybrid, the carbon-cobalt bonds break as early as the strain reaches 5%. By forming a structure without carbon-cobalt bonds, as shown in Fig. 1(f), the metal-CN hybrid maintains in the metastable state until 12% strain. It can sustain against the deformation up to an applied strain of 20% by transforming

[a]Author to whom correspondence should be addressed: Electronic mail: mmzheng@polyu.edu.hk.

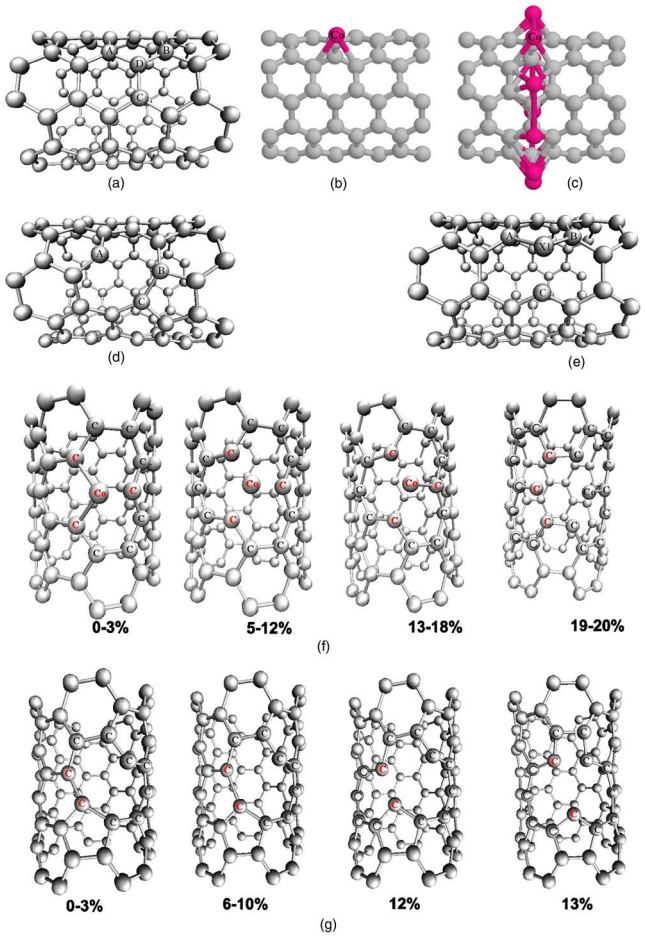

FIG. 1. (Color online) (a) Pristine (5, 5) CN. (b) A defective CN with a cobalt adatom before relaxation. (c) A defective CN with a ring of ten cobalt atoms before relaxation. (d) Stable defective (5, 5) CN with a monovacancy after relaxation. (e) Stable defective (5, 5) CN with a cobalt atom (X1) filling at the vacancy site after relaxation. (f) The structures of cobalt-repaired defective CN under various tensile strains. (g) The structures of defective CN under various tensile strains. Cobalt atoms near the vacancy site are marked in red.

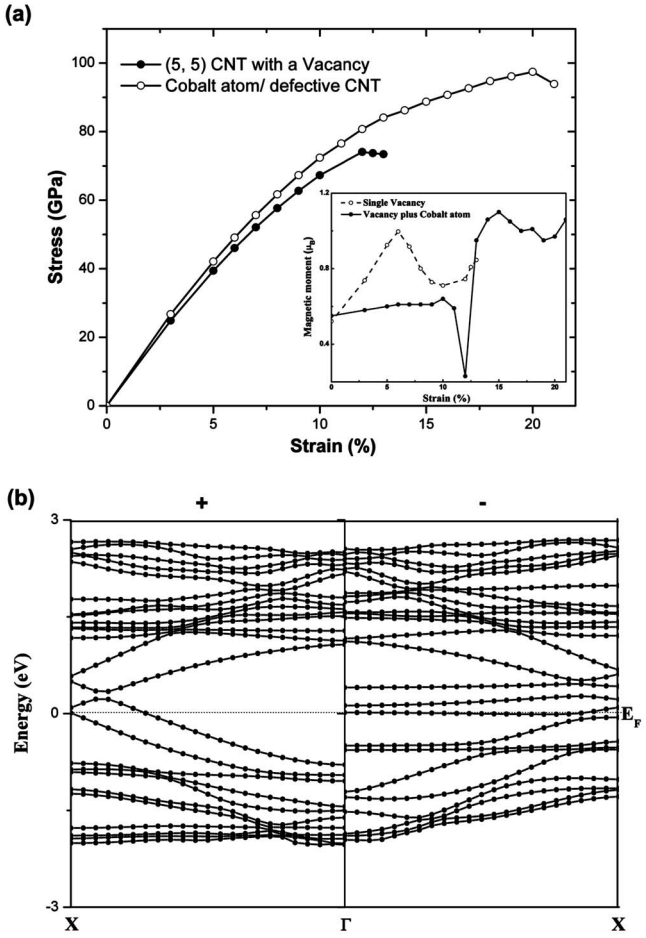

FIG. 2. (a) Tensile stress-strain relations of defective CN and cobalt-repaired defective CN. The inset is the magnetic moments under various strains of deformed defective (5, 5) CN (dash line) and deformed cobalt-repaired defective CN (solid line). (b) Band structure of deformed cobalt-repaired defective CN at 14% strain.

into another structure where different carbon-cobalt bonds form.

Figure 2(a) shows the stress-strain curves for a defective CN and for a metal-CN hybrid structure. The ultimate tensile stress (UTS) of 74.1 GPa appears at a tensile strain of 12% in the former, while it is 98 GPa at a strain of 20% in the latter. The fracture stress can be approximated by the UTS. The ductility ε_L defined as the elongation to failure is approximated as 12.5% and 21% for defective CN and metal-CN hybrid, respectively, when the stress is slightly excess UTS. Young's modulus E fitted from the stress-strain curve at zero strain is $E=0.79$ TPa for defective CN and $E=1.03$ TPa for metal-CN hybrid structure. These discrepancies of mechanical behaviors between defective CN and metal-repaired CN indicate clearly the significantly enhanced mechanical strength and ductility of metal-repaired defective CN.

The strain-dependent magnetic moments are shown in the inset of Fig. 2(a). For metal-repaired CN, the magnetic moment varies around $0.55\mu_B$ when the applied strain is below 12% and suddenly drops to close to zero at 12% strain. The magnetic moment abruptly increases to around $1.0\mu_B$ when the applied strain is larger than 13%, which is analogous to a strain-induced paramagnetic-to-ferromagnetic transition. In defective CN, the magnetic moment gradually changes with strain. Such differences suggest that the deformation-induced magnetization or spin-polarized transition in the metal-CN hybrid structure indicating by a "cusp" in the strain-magnetization curve could be the deformation mechanism for the occurrence of strain hardening especially beyond 12% strain.

To further elucidate the deformation mechanism of metal-repaired defective CN, in Fig. 3(b), we show the isosurfaces of spin densities $\Delta n(\mathbf{r})$ at different strains and with the same isosurface value. Here, $\Delta n(\mathbf{r})$ is computed by the spin-up $(+)$ and the spin-down $(-)$ density at position $\mathbf{r}$. The spin density is slightly polarized along the x direction under an applied strain below 12%. The spin polarization almost diminishes at 12% strain and then its direction suddenly transforms to that is not along the x direction with increasing strain. The strain hardening is accompanied by significantly polarized spin density along the z direction at 14% strain. The spin density fluctuates or flows around the site of substitutional cobalt atom under large applied strains between 14% and 21%. In the case of deformed defective CN, spin polarization shown in Fig. 3(a) indicates that the direction is mainly along the perpendicular bond, which suggests that the magnetomechanical coupling in unrepaired CN is much smaller than that of metal-repaired CN.

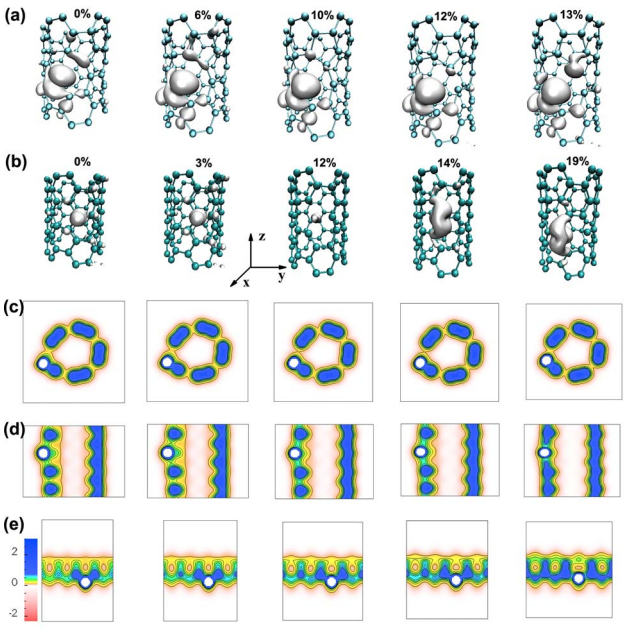

FIG. 3. (Color online) (a) Spin density isosurfaces of unrepaired defective CN. (b) Spin density isosurfaces of metal-repaired defective CN. [(c)–(e)] *XY*-, *XZ*-, and *YZ*-cross-sectional views of charge-density differences plots of the metal-repaired defective CN. Red color indicates charge depletion and other colors denote charge accumulation (in unit of 0.1 $e/\text{Å}^3$).

The charge redistributions shown in Figs. 3(c)–3(e) may unveil the origin of strong magnetomechanical coupling in the deformed metal-CN hybrid structure. The charge redistribution plots can be described by the charge density difference derived from the difference between total charge of metal-CN hybrid and the charge of an isolated carbon atom. Charge transfer to carbon atoms along the axial direction can be observed at the *XZ* and *YZ* cross-sectional planes of the plots especially at a strain larger than 12%. The charge transfer is caused by the effect of strain on the bonds with *p-d* hybridization nature surrounding the substitutional cobalt atom, as demonstrated in the charge difference plots. As shown in Fig. 3(e), the *d*-orbital related wave functions obviously change under large strain. Analytical ferromagnetic Hubbard model[13] has predicted that the less dispersion of energy bands (flat bands) near the Fermi level E_F is essential to the spin polarization in CN with defects or graphite ribbons.[14] Our band structure result shown in Fig. 2(b) supports these theoretical accounts. The band near E_F is very flat when the strain is larger than 13%. In metal-repaired defective CN under a large applied strain, the unbalanced sp^2 hybridization atoms lead to the spin polarization along the zigzag edge or the tube axis of armchair CN. This may explain why the net magnetization tends to align along the tube axis after the charge transfer occurs at high strains, resulting in a strong magnetomechanical coupling.

In summary, the enhanced mechanical strength and ductility of cobalt-repaired defective CN are caused by the strong magnetomechanical coupling which is analyzed by the structural and magnetic transitions, electronic structures, and spin and charge distributions during the tensile test. The issue about how other transition metals affect the mechanical properties of metal-CN hybrid structures deserves further investigations.

The work described in this paper was supported by a grant from the Research Grants Council of the Hong Kong Special Administrative Region, China (Project No. PolyU 7195/07E).

[1]Y. Fan, B. R. Goldsmith, and P. G. Collins, Nat. Mater. **4**, 906 (2005).
[2]M. F. Yu, B. S. Files, S. Arepalli, and R. S. Ruoff, Phys. Rev. Lett. **84**, 5552 (2000).
[3]L. B. da Silva, S. B. Fagan, R. Motal, and A. Fazzio, Nanotechnology **17**, 4088 (2006).
[4]A. Kis, T.-N. Lee, E. Couteau, A. J. Kulik, W. Benoit, L. Forró, G. Csányi, J.-P. Salvetat, and J. Brugger, Nat. Mater. **3**, 153 (2004).
[5]S. Namilae, N. Chandra, and C. Shet, Chem. Phys. Lett. **387**, 247 (2004); A. Garg and S. B. Sinnott, *ibid.* **295**, 273 (1998).
[6]S. H. Yang, W. H. Shin, J. W. Lee, H. S. Kim, J. K. Kang, and Y. K. Kim, Appl. Phys. Lett. **90**, 013103 (2007).
[7]S. I. Cha, K. T. Kim, S. N. Arshad, C. B. Mo, and S. H. Hong, Adv. Mater. (Weinheim, Ger.) **17**, 1377 (2005).
[8]P. M. Ajayan and J. M. Tour, Nature (London) **477**, 1066 (2007).
[9]G. Kresse and J. Furthmüller, Phys. Rev. B **54**, 11169 (1996).
[10]G. Kresse and J. Joubert, Phys. Rev. B **59**, 1758 (1999).
[11]Y. Ma, P. O. Lehtinen, A. S. Foster, and R. M. Nieminen, New J. Phys. **6**, 68 (2004); W. Orellana and P. Fuentealba, Surf. Sci. **600**, 4305 (2006).
[12]Y. Yagi, T. M. Briere, M. H. F. Sluiter, V. Kumar, A. A. Farajian, and Y. Kawazoe, Phys. Rev. B **69**, 075414 (2004).
[13]H. Tasaki, Phys. Rev. Lett. **69**, 1608 (1992); Prog. Theor. Phys. **99**, 489 (1998).
[14]T. L Makarova, Semiconductors **38**, 615 (2004).